Bulletin of the JSME, Vol.19, No.132 June, 1976

621.833.6

Dynamic Behavior of Planetary Gear

(1st Report Load Distribution in Planetary Gear)

By Teruaki HIDAKA and Yoshio TERAUCHI

In the planetary gear, the inequality of load distribution arises on each planet gear because of random errors of manufacture and assembly. This phenomenon results in an increase of load to each part, the occurrence of vibration, and a drop in efficiency of planetary gear systems. Though there are a number of studies which are connected with load distribution, many of them are static studies. However, in fact, the dynamic behavior of load distribution in driving is complicated because of the influence of the deformation in each part, dynamic characteristic of the system. Therefore, to explain these relations, a systematic experimental work was carried out using Stoekicht planetary gear(Type 2K-H) with spur gears.

Consequently, the following items are explained in this paper: (i) The mean values of load distribution among the planetary gears are nearly equality, but variations of dynamic tooth loads grow large in the high-speed range. (ii) Even if load distribution is equality, it happens that gear tooth dynamic loads vary largely.

1. Introduction

The planetary gear have the following advantages:

1.The planetary gear have more compact size,higher efficiency and larger speed-ratio in comparison with the parallel-shaft gear.

2. The planetary gear are coaxial. This feature allows simple controls for speed changing applications. Clutches and brakes permit rapid speed changing without taking the gears out of mesh.

The inequality of the load distribution, however, arises on each planet gear in the planetary gear because of random errors of manufacture and assembly. This phenomenon results in an increase of load on each part, the occurrence of vibration, and a drop in efficiency of planetary gear systems. The seizure may arise on the planet spindles by the influence of inertia force of planet gears in the high-speed range, through lubrication. Due to these phenomena, there are many problems to be overcome to make good use of the advantages of the planetary gear. It is the most important of all the problems to carry out the equalization of the load distribution among planet gears. So far, for the equalization of the load distribution various methods have been considered by many investigations, and there have been many theoretical investigation.[1]

Received 27th August, 1974.

Lecturer, Faculty of Engineering, Hiroshima University, 3 Sendamachi Hiroshima.
Professer, Faculty of Engineering, Hiroshima.

However, experimental investigations in driving are few, because the mechanism of the planetary gear is complicated.

In recent studies connected with the load distribution, B.Dizioglu[2] expressed the conditional equations for the equalization of the load distribution under the static and dynamic conditions by replacing the planetary gear having three planet gears with the link mechanism. D.E.Imwalle[3] classified the planetary gear from a standpoint of the load distribution, and explained the dynamic loads acting on planet gears with a simple expression containing the term of inertia, but he took no account of the important elastic deformation in each part of the planetary gear. Hayashi, et al.[4] carried out an analysis of the static load balancing in the normal plane to the gear axis for single-stage planetary gear system, and then derived the conditions and the basic equation for the load balancing by replacing the geometrical errors of each gear, the errors caused by the gap in the bearing and by the elastic deformation with the equivalent tooth surface errors and the equivalent displacements, and further, investigated various methods for the load balancing. However, all of their studies were not expermental investigations. Yu.D. Kondrashov[5] carried out expermental investigation using the Type 2K-H planetary gear(single-stage type) in the low-speed region. From the measured results he explained that the equalization of the load distribution among planet gears was fulfilled by using a floating sun gear in combination with sphercal-race bearing on the planet gears, but the use of a floating ring gear did not very effectively

equalize the load among planet gears. However, in fact, the dynamic behavior of the load distribution in driving is very complicated, because it is influenced by the operational characteristics of the planetary gear, such as the external load, the variation of torque, the vibration characteristics of the system, and by the errors of manufacture and assembly. Therefore, to explain the problems on the operational performance of the planetary gear, in particular the problem of the dynamic behavior, a systematic experimental investigation has been carried out using single-stage Stoekicht planetary gear(Type 2k-H) with spur gears, which is a most general planetary gear system. The gear testing machine used is of the power circulating type.

In this paper, the measured results and the consideration connected with the load distribution for the planetary gear in driving are described.

2. Measuring Apparatus and Experimental Procedure

2.1 Measuring Apparatus

Fig.1 shows the gear testing machine with a planetary gear①, which is of power circulating type. This testing machine is 5m in full length, in which a 20KW induction motor② with a Kopp type stepless speed variator is used for the drive. The machine was designed for the maximum circulating power of 110KW, a speed range to the higher speed shaft of the planetary gear from 1740rpm to 8900rpm, or from 3500rpm to 17800rpm(by exchanging two sets of the power return gears⑤). On the other hand, by means of the 1.5KW motor⑦ with reduction gears, the planetary gear can be driven at a very slow speed of 18rpm. The higher speed shaft was bored in the direction of its axis in order to pass the measuring wires there through. For this reason the length of the shaft is desirably not to be very long, but it was designed as long as possible, i,e., 450mm so as not to be affected by the speed change gear③ for the planetary gear. The speed change gear was designed for the structure for which it is possible to arrange the slip-ring④ at an end of the higher speed shaft. The mesh-frequency was indicated with the aid of photoelectric pulses being generated by means of the toothed index disk⑩ on the lower speed shaft of the planetary gear. For the lubrication in the planetary gear a hydraulic pump was used, and the higher speed shaft bearings with the single row ball bearing were lubricated by means of the forced fog lubrication.

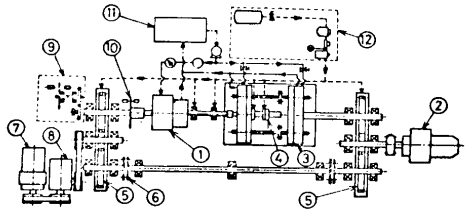

1 planetary gear
2 Kopp type stepless speed variator
3 speed change gears
4 slip-ring
5 power return gear
6 loading device
7 motor
8 reduction gears
9 synchronous device
10 index disk
11 oil tank
12 lubricating device

Fig.1 Power circulating type gear testing machine

2.2 Tested Planetary Gear

The Stoekicht type single-stage planetary gear(Type 2K-H) is shown in Fig.2. This planetary gear with spur gears was designed for the nominal transmitted power 20KW, the speed ratio 6 and the working range of the higher speed shaft from 1800-rpm to 7200rpm. The geometries, the materials and the gear accuracies of the planetary gear are shown in Table 1, and Fig.3 shows the shaft diameters and the gaps between the shaft and the bearing in the planetary gear. The tooth profile errors and the lead errors are represented in Fig.4 for the sun gear and the planet gear. It is for the purpose of avoiding the experimental error caused by the unevenness of gear contact pattern that the sun gear has a large crowing.

2.3 Experimental Procedure

It is difficult to measure the load distribution on each planet gear directly,

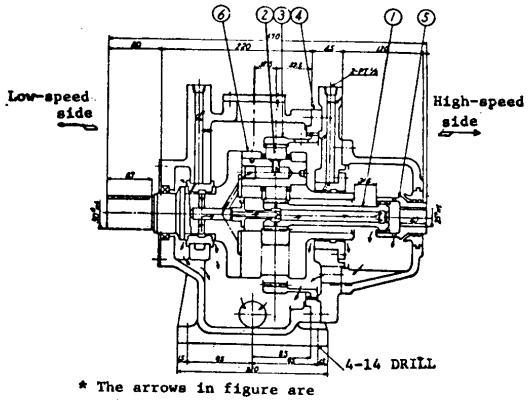

* The arrows in figure are the direction of flowing oil.

1 sun gear
2 planet gear
3 ring gear
4 coupling retainer
5 high-speed gear coupling
6 planet carrier

Fig.2 Stoekicht type planetary gear

Table 1 Dimensions and accuracies of planetary gear

	Sun gear	Planet gear			Ring gear	Planet carrier
Number of teeth	14	28			70	—
Radius of pitch circle mm	21.000	42.000			105.000	—
Radius of base circle mm	19.401	38.803			97.007	—
Face width mm	30	30			36	—
Material	Nitriding steel	Nitriding steel			SCM2	S30C
Thickness of ring mm	—	—			8.65	—
Single pitch error μ	2.4(0)	5(1)	5(1)	5(1)		—
Pitch variation μ	3(0)	6(0)	6(0)	4(0)		—
Accumulative pitch error μ	3(0)	14(0)	28(2)	17(0)		—
Tooth profile error μ	3(0)	4(0)	5(1)	6(1)		—
Lead error μ	4(0)	5(0)	7(0)	6(0)		—
Amount of crowning μ	30	15			—	—
Normal backlash mm	0.14	0.17				—

Dedendum	1.25m	Module m	3
Addendum	0.9 m	Pressure angle	22.5°
Addendum modification coefficient	0	Speed ratio	6

Numbers in the brackets are the grade for JIS.

because the planet gears turn round on their own axis, and also revolve round the sun gear. Therefore, the tooth loads on the sun gear were measured from the fillet strains in the three teeth(tooth numbers 1, 5 and 10) of the sun gear, which engage simultaneously with the three planet gears respectively. The fillet strains were detected by means of the resistance wire strain gauges which were stuck on the compression sides of roots of the three teeth. The strain gauges were stuck with great care, so that the discrepancy among the positions of the three gauges was less than 0.3mm. Fig.5 shows the electric circuit diagram. The electric signal from the three strain gauges is transmitted through the slip-ring, the bridge circuit and the DC amplifier. The output signal from the DC amplifier is once recorded on the magnetic tape in date-recorder. During the recording the signal is observed by means of an oscilloscope. The fillet strain data in the data-recorder are recorded again on the pen type oscillograph, after the time scale of the fillet strain has been extended to 400 times by using two data-recorders. At this time the pitch signal and the synchronizing signal are also recorded. Fig.6 shows a diagram of the engaging state in the planetary gear for the case of the reduction and the observation from the side of the lower speed shaft. If the planet gears and the teeth of each gear are numbered as shown in this figure, the synchronous position will be such that the planet gear Pℓ 1 lies right above, that is, the tooth No.70(the tooth No.1 for the speed-up) of the ring gear engages with the tooth No.1 of the planet gear Pℓ 1. At this time the three teeth No.1, No.5 and No.10 of the sun gear engage with the planet gears Pℓ 1, Pℓ 2 and Pℓ 3 respectively. From the relation between the numbers of teeth shown in Table 1, if the lower speed shaft(planet carrier shaft) rotates 2 times, thus, the higher speed shaft rotates 12 times, it will be reduced to the very same engaging state as before. As the difference of the rotation between the higher speed shaft and the lower speed shaft is 10 times, in an interval from one synchronous position to next synchronous position a certain tooth of the sun gear engages 30 times with the three planet gears, thus, the fillet strains of the three teeth No.1, No.5 and No.10 amount to 90 pieces in all. These fillet strains are a set of data. The measurement of the dynamic fillet strain was carried out at intervals of the mesh-frequency of 40Hz for the working range of the higher speed shaft from 1740rpm to 7200rpm(the mesh-frequency range from 334Hz to 1400Hz). On the other hand, 90 pieces of static fillet strains in an interval from one synchronous position to next synchronous position were also measured by driving the planetaly gear drive very slowly by means of the motor⑦ with reduction gears shown in

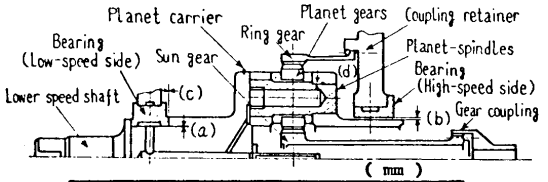

(mm)

	Designation		Shaft diameter	Gap
a	Bearing (low-speed side)		φ60	0.09
b	Bearing (High-speed side)		φ70	0.008
c	Thrust bearing		φ45	0.20
d	Planet-spindle	Pℓ 1	φ40	0.13
		Pℓ 2		0.10
		Pℓ 3		0.12

1 The dimensions of a,b and d are the diametral gap.
2 The dimension of c is the gap which equals the right gap plus the left gap.

Fig.3 Shaft diamaters and gaps between shaft and bearing

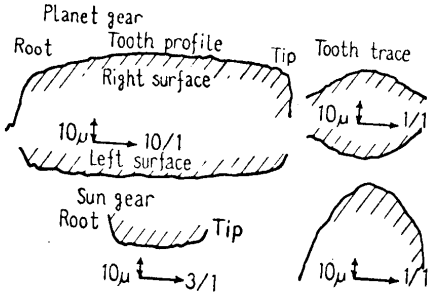

Fig.4 Tooth profile errors and lead errors of sun gear and planet gear

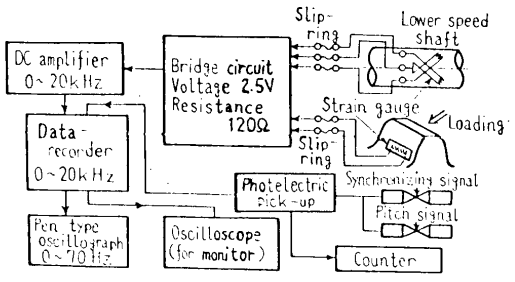

Fig.5 Diagram of electric circuit

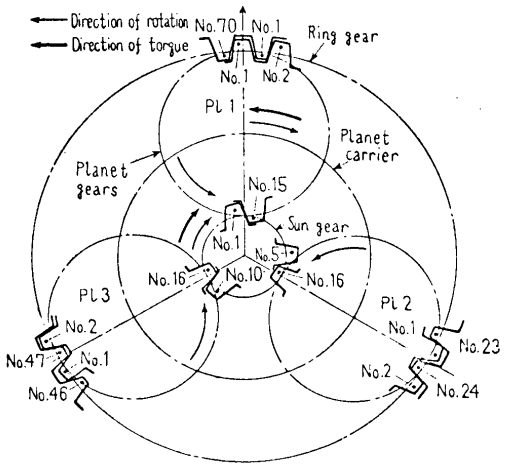

Fig.6 Diagram of engaging state in planetary gear

Fig.1. As a characteristic value for the dynamic teeth loading a so-called dynamic load factor was introduced, which was defined as the ratio of a dynamic fillet strain to a static fillet strain in the position corresponding with the measured position of the dynamic strain. Also, the reproducibility of the fillet strains was confirmed, because 90 pieces of the fillet strains between two synchronous positions corresponded with those between next synchronous positions respectively. As shown in the electric circuit diagram (Fig.5), the variation of torque was also measured and, further, was compared with the dynamic tooth load.

In order to confirm the degree of the experimental error caused by the unevenness of gear contact pattern abovemeantioned, the fillet strains in the three positions which were the middle of face width and each 13.5mm of both sides from the middle, were measured, and the fillet strain distribution in the direction of tooth trace was approximated with a parabola which was composed of three values of the measured fillet strains. The following results were obtained by evaluating the difference between the obtained maximum strain from the approximated strain distribution and an actual fillet strain in the middle position of face width: the difference on the average was 1%, and the maximum difference was less than 5%. Therefore, it may be considered that the dynamic tooth load can be measured from the fillet strain in the middle position of face width.

3. Calculation Method of Load Distribution on Each Planet Gear

There are a number of methods for the measurement of the load distribution on each planet gear, such as measuring the reaction force on the planet spindle and measuring the fillet strain of each gear, but these methods have the advantage and disadvantage. To measure the fillet strain of the non-rotating ring gear is easy, but in the ring gear of the toothed thin-ring the strain is caused by the ring deformation, and for this reason the measuring accuracy is not satisfactory. As described in this paper, to estimate the load distribution from fillet strains of the sun gear is equal to predicting the distribution of the dynamic loads on each planet gear. As the reproducibility of the fillet strains was confirmed as abovementioned, the load distribution was estimated by measuring the dynamic loads on the sun gear in a certain interval between two synchronous positions. At this time, it was to be desired that the loads on all the teeth of the sun gear should be measred at the same time, but in this paper the loads on the three teeth of No.1, No.5 and No.10 were measured. In order to estimate the load distribution and the dynamic tooth load, the following calculation procedure was applied to the date of 90 pieces of the fillet strain. Further, in the next section the resuls of the dynamic tooth load and the load distribution will be discussed.

Now, the notations are as follow:

i_s = numbers of measured teeth on the sun gear(in this paper, = 1, 5, 10)

j = number of times at which a tooth of sun gear engages with the teeth of each planet gear in an interval between two synchronous positions(= 30 in this paper)

$\varepsilon_{0s}(i_s,j)$: static fillet strain of the sun gear

$\varepsilon_{ds}(i_s,j)$: dynamic fillet strain of the sun gear

$W_{0s}(i_s,j)$: static load of the sun gear (transmitted load)

$W_{ds}(i_s,j)$: dynamic load of the sun gear

$w_{ds}(i_s,j)$: dynamic load factor for the sun gear

As $\varepsilon_{0s}(i_s,j)$ and $\varepsilon_{ds}(i_s,j)$ are the strains in the same mesh point, the expressions for $w_{ds}(i_s,j)$ and $W_{ds}(i_s,j)$ may be found as follows.

$$w_{ds}(i_s,j)=\varepsilon_{ds}(i_s,j)/\varepsilon_{0s}(i_s,j) \quad \cdots\cdots(1)$$

$$W_{ds}(i_s,j)=w_{ds}(i_s,j)W_{0s}(i_s,j) \quad \cdots\cdots(2)$$

For the teeth No.1, No.5 and No.10 of the sun gear which engage simultaneously with the three planet gears respectively, the mean dynamic load factor $\bar{w}_{ds}(i_s)$ can be given as

$$\bar{w}_{ds}(i_s)=\frac{1}{30}\sum_{j=1}^{30} w_{ds}(i_s,j) \qquad i_s=1,\ 5,\ 10 \quad \cdots\cdots(3)$$

Further, the standard deviation $\sigma_{wds}(i_s)$ which expresses the dispersion in the dynamic load factors, is written as follows:

$$\sigma_{wds}(i_s)=\sqrt{\frac{1}{30}\sum_{j=1}^{30} w_{ds}^2(i_s,j)-\bar{w}_{ds}^2(i_s)} \quad \cdots\cdots(4)$$
$$(i_s=1,\ 5,\ 10)$$

The coefficient of variation $C_{wds}(i_s)$ representing the rate of this standard deviation to the mean value, can be given as

$$C_{wds}(i_s)=\{\sigma_{wds}(i_s)/\bar{w}_{ds}(i_s)\}\times 100\% \quad \cdots\cdots(5)$$
$$(i_s=1,\ 5,\ 10)$$

Also, the load distribution rate $Q_s(i_s,j)$ for the three teeth No.1, No.5 and No.10 which engage at the same time, may be found as follows:

$$Q_s(i_s,j)=\left\{w_{ds}(i_s,j)\Big/\frac{1}{3}\sum_{i_s}^{1,5,10} w_{ds}(i_s,j)\right\}\times 100\% \qquad (i_s=1,\ 5,\ 10) \quad \cdots\cdots(6)$$

where $Q_s(i_s,j)$ is 100% in case of the equal loads. Just as in the case of the dynamic load factor, the mean load distribution rate $\bar{Q}_s(i_s)$ for the three teeth of the sun gear, its standard deviation $\sigma_{Qs}(i_s)$ and the coefficient of variation $C_{Qs}(i_s)$ are given by the following expression, respectively:

$$\bar{Q}_s(i_s)=\frac{1}{30}\sum_{j=1}^{30} Q_s(i_s,j) \quad \cdots\cdots(7)$$

$$\sigma_{Q_s}(i_s)=\sqrt{\frac{1}{30}\sum_{j=1}^{30}Q_s^2(i_s,j)-\bar{Q}_s^2(i_s)} \quad \cdots\cdots(8)$$

$$C_{Q_s}(i_s)=\{\sigma_{Q_s}(i_s)/\bar{Q}_s(i_s)\}\times 100\% \quad \cdots\cdots(9)$$

$$(i_s=1,\ 5,\ 10)$$

Next, as the tooth loads on the sun gear are equal to those on the planet gears, putting $\bar{w}_{dp}(i_p)$, $i_p=1,\ 2,\ 3$ as the mean dynamic load factor for the three planet gears Pℓ 1, Pℓ 2 and Pℓ 3, the following expressions can be obtained:

For the case of the present paper:

$$\left.\begin{aligned}
\bar{w}_{dp}(1)&=\frac{1}{30}\Big\{\sum_{k=1}^{10}w_{ds}(1,3k-2)+\sum_{k=1}^{10}w_{ds}(5,3k)\\
&\quad+\sum_{k=1}^{10}w_{ds}(10,3k-1)\Big\}\\
\bar{w}_{dp}(2)&=\frac{1}{30}\Big\{\sum_{k=1}^{10}w_{ds}(1,3k-1)+\sum_{k=1}^{10}w_{ds}(5,3k-2)\\
&\quad+\sum_{k=1}^{10}w_{ds}(10,3k)\Big\}\\
\bar{w}_{dp}(3)&=\frac{1}{30}\Big\{\sum_{k=1}^{10}w_{ds}(1,3k)+\sum_{k=1}^{10}w_{ds}(5,3k-1)\\
&\quad+\sum_{k=1}^{10}w_{ds}(10,3k-2)\Big\}
\end{aligned}\right\}(10)$$

The standard deviation $\sigma_{wdp}(i_p)$, and the coefficient of variation $C_{wdp}(i_p)$, $i_p=1,\ 2,\ 3$ can be also obtained in the same manner.

Further, the mean load distribution rates $\bar{Q}_p(i_p)$ for the three planet gears Pℓ 1, Pℓ 2 and Pℓ 3, are:

$$\left.\begin{aligned}
\bar{Q}_p(1)&=\frac{1}{30}\Big\{\sum_{k=1}^{10}Q_s(1,3k-2)+\sum_{k=1}^{10}Q_s(5,3k)\\
&\quad+\sum_{k=1}^{10}Q_s(10,3k-1)\Big\}\\
\bar{Q}_p(2)&=\frac{1}{30}\Big\{\sum_{k=1}^{10}Q_s(1,3k-1)+\sum_{k=1}^{10}Q_s(5,3k-2)\\
&\quad+\sum_{k=1}^{10}Q_s(10,3k)\Big\}\\
\bar{Q}_p(3)&=\frac{1}{30}\Big\{\sum_{k=1}^{10}Q_s(1,3k)+\sum_{k=1}^{10}Q_s(5,3k-1)\\
&\quad+\sum_{k=1}^{10}Q_s(10,3k-2)\Big\}
\end{aligned}\right\}(11)$$

$\sigma_{Qp}(i_p)$ and $C_{Qp}(i_p)$, $i_p=1,\ 2,\ 3$ can be also obtained in the same manner.

Fig.7 shows the engagement relation among the three planet gears. For the above-mentioned calculation procedures, the following two means were applied to the data of the fillet strains. It is explained from Fig.7 that the meshing position in which the teeth No.1, No.5 and No. 10 of the sun gear engage at the same time, and which is the zone of single contact, is nearly tip on the tooth No. 1, nearly root on the tooth No.5 and nearly pitch point on the tooth No.10(see Fig.8 also). Thus, the estimation of the load distribution was carried out at this meshing position. Further, the estimation of the dynamic load was carried out at the meshing position other than the above-mentioned one.

4. Experimental Results and Discussion

4.1 Experimental Condition

The experimental investigation was carried out at a transmitted tooth load 130kg(a higher speed shaft torque 7.7kg-m, a transmitted power 57KW at the maximum speed) for the case of the reduction. The results of the experimental investigation are expressed as follows.

4.2 Static Load on Gear

Fig.8 shows an example of the fillet strain for the case of driving the planetary gear at a very slow speed of 18rpm. 30 pieces of the fillet strains between two synchronous positions for the respective teeth were nearly the same form, further, the coefficient of variation of the maximum fillet strains was about 3%. This dispersion can deservedly be explained also for the fillet strains of the parallel-shaft gear devices because of the gear errors. Also, taking into consideration the discrepancy among the positions of the three stuck gauges, there is little difference among the fillet strains of No.1, No.5 and No.10. Thus, in case of driving at a very slow speed, it is considered that the equalization of the load distribution is fully fulfilled. Therefore, regarding the above-mentioned fillet strain as the static fillet strain of the sun gear(for $W_{0s}(i_s,j)$ = constant = W_0 = 130kg), the dynamic load factor and the load distribution were estimated.

4.3 Dynamic Load on Gear

Figs.9 and 10 show an example of the fillet strains which are measured at the mesh-frequencies 334Hz and 1400Hz, respectively. In the high-speed range the dynamic tooth load is vibrational as shown in Fig.10. However, no hasty increase of the dynamic loadings arises, because no release of the teeth occurs and no teeth contact impulsively. In order to investigate the effect of the meshing position on the dynamic loading, the mean values of dy-

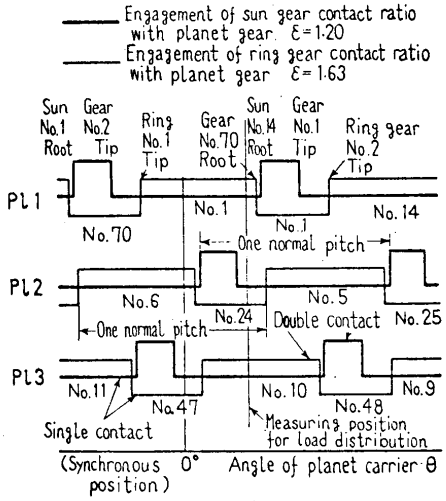

Fig. 7 Engagement relation among three planet gears

namic load factor $\bar{w}_{ds}(i_s)$ at the meshing positions of the tooth tip, the tooth root and pitch point in the zone of single contact were estimated, and are shown in Fig.11. From this figure it is seen that the dynamic load factors grow large in order of the tooth root, the tooth tip and the pitch point with an increasing speed. This phenomenon can be explained by dynamic additional loads which occur due to the change of teeth stiffness as a result of the different contact teeth numbers(i. e. single contact or double contact). However, as the dynamic load factors of the three teeth of No. 1, No.5 and No.10 are similarity, it is guessed that the load distribution is nearly equality. In this paper, from the maximum fillet strains the mean dynamic load factor $\bar{w}_{ds}(i_s)$ and the coefficient of variation $C_{wds}(i_s)$ were estimated. The results are shown in Fig.12. From this figure it is recognized that the mean values of the dynamic load factor do not widely vary, but the coefficients of variation differ from mesh-frequency to mesh-frequency. Therefore, the dispersions in the dynamic loads for the specially fixed mesh-frequencies are shown in Fig. 13 with the relation between dynamic load factor and angle of rotation of the lower speed shaft. At a low speed(mesh-frequency 480Hz) at which the coefficient of variation is large, the dynamic loads make regu-

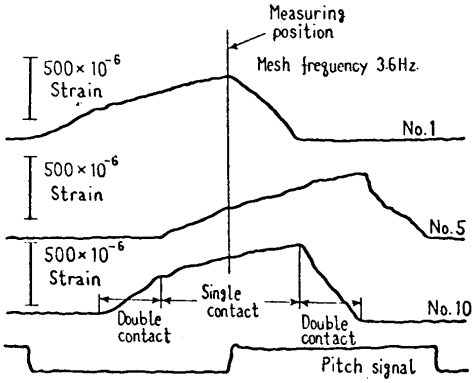

Fig. 8 Example of fillet strain

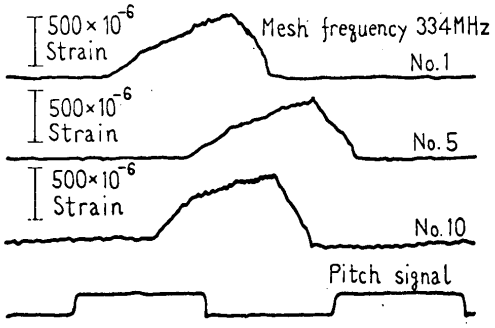

Fig. 9 Example of fillet strain

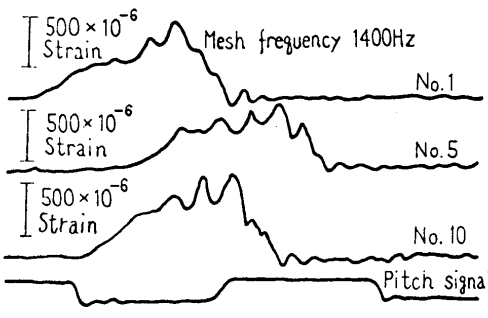

Fig. 10 Example of fillet strain

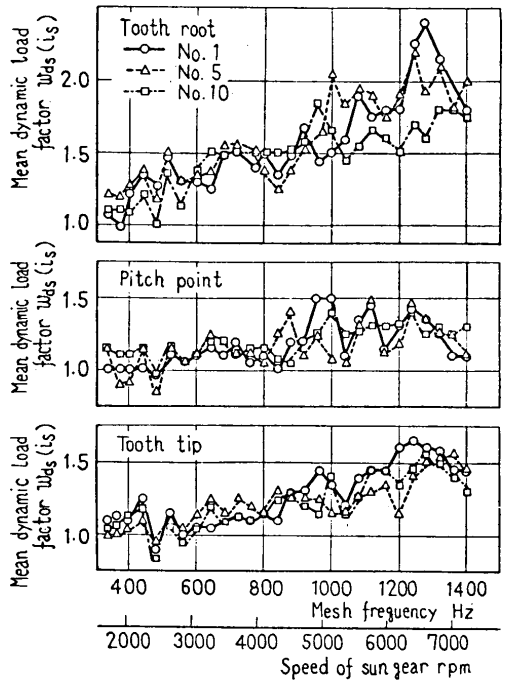

Fig. 11 Dynamic load factors for tooth root, pitch point and tooth tip

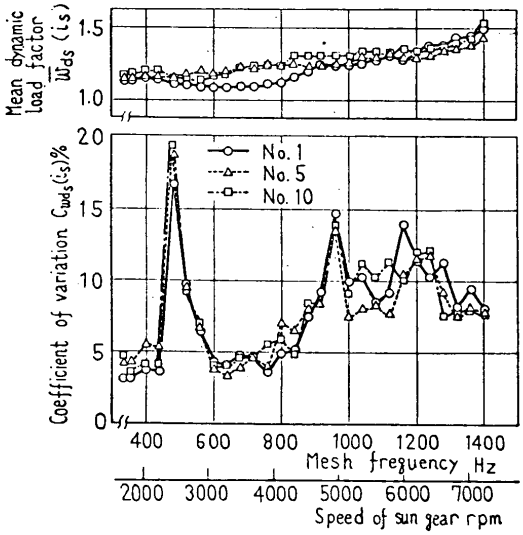

Fig. 12 Mean dynamic load and coefficient of variation

lar periodic variations under the equal load distribution, while at a high speed (mesh-frequency 1400Hz) they vary irregularly under the unequal distribution. When the torque of the lower speed shaft was measured, it was revealed that the torque variation had 12 periods per rotation of the lower speed shaft at the mesh-frequency 480Hz and 6 periods at 960Hz, and then the resonances occurred in the gear testing machine. The cycles of these torque variations are shown in Fig.13 with the dotted lines. Seeing only the plotted points for dynamic load factors in Fig.13, it seems that there are the periodic variations of 3 times per rotation of the lower speed shaft at 480Hz. The reason is that the number of the measured root strains is too few. If the measurement is carried out for all the teeth, 12 pieces of peaks ought to arise.

In case of measuring the fillet strains at the same time compared with Fig.12 the mean dynamic load factors $\bar{w}_{ds}(i_s)$, $\bar{w}_{dp}(i_p)$ are slightly small and the coefficients of variation $C_{wds}(i_s)$, $C_{wdp}(i_p)$, are slightly large, but, these graphs are similar to Fig.12 as a whole(the figures are omitted).

4.4 Load Distribution

The mean load distribution rate $\bar{\Omega}_s(i_s)$ and the coefficient of variation $C_{\Omega s}(i_s)$ are shown in Fig.14, which are estimated by measuring the three fillet strains at the same time as above-mentioned. Similarly, $\bar{\Omega}_p(i_p)$ and $C_{\Omega p}(i_p)$ are shown in Fig.15 . Comparing Fig.14 with Fig.15, the mean load distribution rate $\bar{\Omega}_s(i_s)$ in Fig.14 fluctuates slightly with an increasing speed, but $\bar{\Omega}_s(i_s)$ in Fig.15 is about 100%. Both the coefficients of variation show a similar tendency, but $C_{\Omega p}(i_p)$ is larger than $C_{\Omega s}(i_s)$. Thus, even if the same measured values are used in both calculations, due to the two different calculation procedures the mean load distribution rate and the

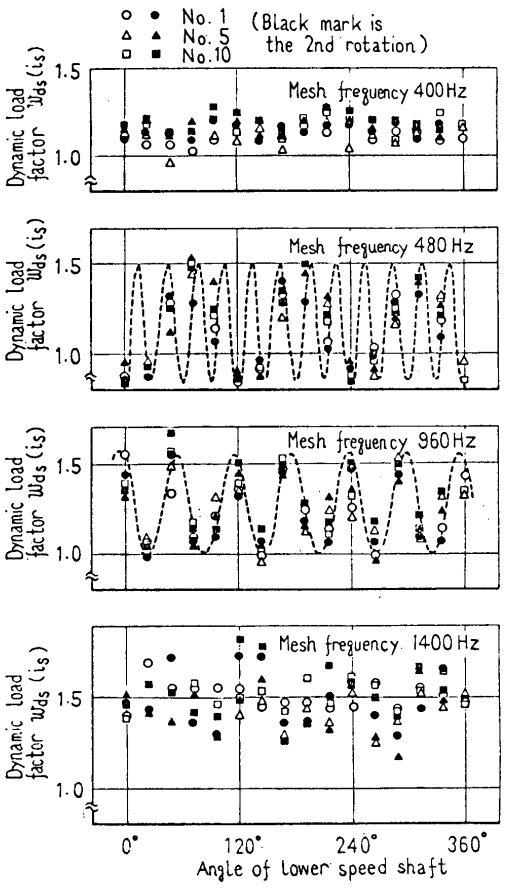

Fig. 13 Relationship between dynamic load and angle of lower speed shaft

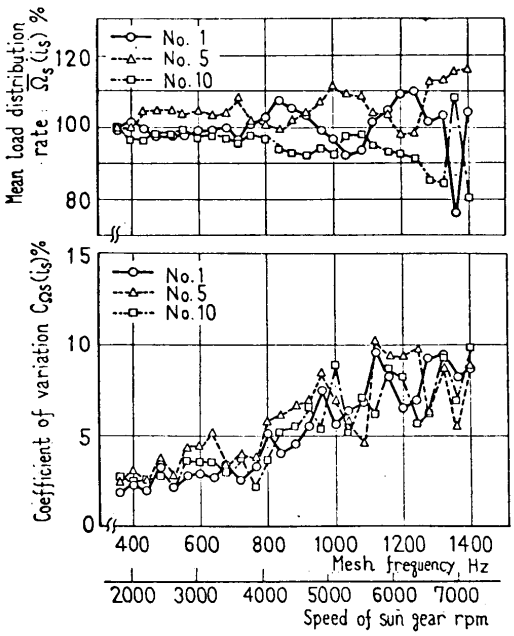

Fig. 14 Mean load distribution rate and coefficient of variation

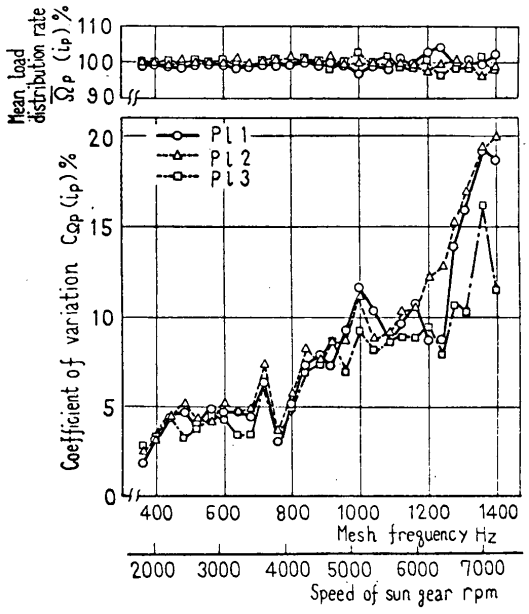

Fig. 15 Mean load distribution rate and coefficient of variation for planet gears

coefficient of variation for the planet gears differ from those for the teeth of the sun gear. Fluctuation of $\bar{Q}_s(i_s)$ is due to the variation of the dynamic tooth load (see Fig.10). In this paper, it is judged that $\bar{Q}_p(i_p)$ expresses the nomal conditions of the load distribution better.

At the mesh-frequency 480Hz, the curve for the coefficient of variation of the dynamic load factors in Fig.12 shows a pointed peak, but the curve for the coefficient of variation of the load distribution rate in Fig.14 has not such a peak. This means that though the load distribution is equality, the variation of dynamic loading is large due to the torque variation. Therefore, the dynamic tooth load can be estimated with only the load distribution rate.

4.5 Mean Value and Coefficient of Variation

Expressing the dynamic loads in Fig.12 with the frequency distribution about the mean values, Fig.16 can be obtained. Though the frequency distribution differs from mesh-frequency to mesh-frequency, most of the dynamic loads are within the range of $[\bar{W}_{ds}(i_s) \pm 2\sigma_{Wds}(i_s)]$. This can be also true for the load distribution.

Thus, if transmitted load W_0 is determined, the dynamic tooth loads $W_{ds}(i_s,j)$, and $W_{dp}(i_p,j)$ may be within the ranges of the following expressions, respectively:

$$\left.\begin{aligned} W_{ds}(i_s,j) &= \bar{W}_{ds}(i_s)\{1 \pm 2C_{Wds}(i_s)/100\}W_0 \\ W_{dp}(i_p,j) &= \bar{W}_{dp}(i_p)\{1 \pm 2C_{Wds}(i_p)/100\}W_0 \end{aligned}\right\} \quad \cdots\cdots\cdots\cdots(12)$$

For example, as the coefficient of variation for a mesh-frequency 1200Hz in Fig.12 is $C_{Wds}(i_s) = 12\%$, the maximum dynamic load may be estimated as follows:

$$1.3\times(1+2\times 0.12)\times 130\,\mathrm{kg} \fallingdotseq 210\,\mathrm{kg}$$

For the load distribution rates $Q_s(i_s,j)$ and $Q_p(i_p,j)$ the following expressions can be obtained in the same manner:

$$\left.\begin{aligned} Q_s(i_s,j) &= \bar{Q}_s(i_s)\{1 \pm 2C_{Qs}(i_s)/100\} \\ Q_p(i_p,j) &= \bar{Q}_p(i_p)\{1 \pm 2C_{Qp}(i_p)/100\} \end{aligned}\right\} \quad \cdots\cdots(13)$$

Thus, the maximum and the minimum value of the load distribution rate for a mesh-frequency 1200Hz in Fig.14 are:

$$110(1+2\times 0.065) \fallingdotseq 124\%$$

$$92(1-2\times 0.075) = 78\%$$

for $i_s = 1_{(max)}$ $i_s = 10_{(min)}$

Further, the mean load distribution rate for 1200Hz in Fig.15 is about 100% regardless of i_p,

$$100(1 \pm 2\times 0.1) = 80\% \sim 120\%$$

Therefore, it can be said that Fig.14 coincides nearly with Fig.15.

5. Conclusions

The conclusions of this paper are summarized as follows:

(1) In the high-speed range the variation of dynamic tooth loads becomes larger, and the load distribution is reduced to inequality.

(2) Even if the load distribution is equality, due to the torque variation it happens that the dynamic tooth loads vary largely. Therefore, the dynamic tooth load can not be estimated from only the mean load distribution rate and the mean dynamic load factor.

(3) The mean load distribution rates for each planet gear are about 100% over the whole speed range, thus, the load distribution for each planet gear is equality. However, though the mean load distribution rates estimated for the three teeth of the sun gear are nearly 100% in the low-speed range, in the high-speed range they fluctuate slightly. Thus, even if the same measured value is used in both calculations, due to the two different calculation procedures the mean load distribution rate and the coefficient of variation for the planet gears differ from those for the teeth of the sun gear.

(4) The ranges of the dynamic tooth loads and the load distributions can be expressed with these mean values and coefficients of variation, respectively.

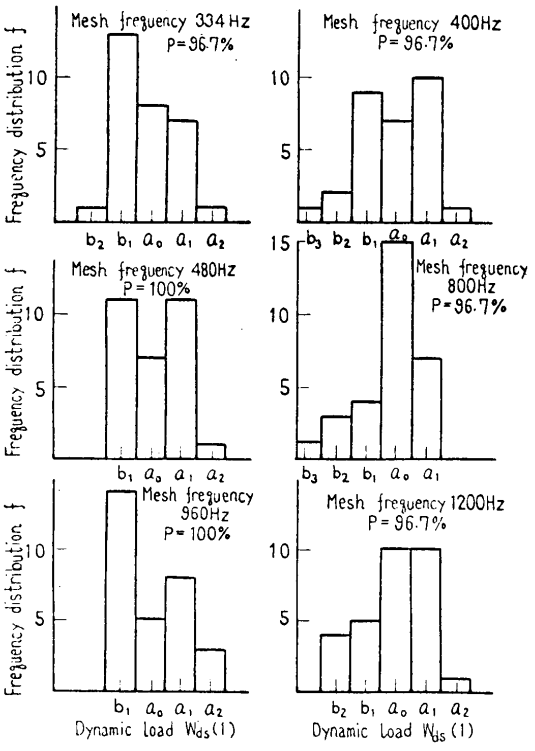

Fig. 16 Frequency distribution of dynamic tooth loads about mean value

References

(1) Senda, M., Gears. (in Japanese), Vol. 10, (1967), p. 3993, Industrial Daily News Co., Ltd.
(2) Dizioglu, B., VDI-Ber, Bd. 167 (1971), s. 193.
(3) Imwalle, D. E., ASME paper, No. 72-PTG-29 (1972-10), p. 1.
(4) Hayashi, T., et al., Trans. Japan Soc. Mesh. Engrs. (in Japanese), Vol. 36, No.288 (1970-8), p.1394.
(5) Kondrashov, Yu. D., Russian Engng. J., Vol. 52, No.10(1972-10), p.30.